

## Effect of crystallization rate on the formation of the polymorphs of solution cast poly(vinylidene fluoride)

Rinaldo Gregorio, Jr. <sup>\*</sup>, Daniel Sousa Borges

Department of Materials Engineering, Federal University of São Carlos, Rod. Washington Luís, Km 235, 13565-905 São Carlos, Sao Paulo, Brazil

### ARTICLE INFO

#### Article history:

Received 16 May 2008

Received in revised form 4 July 2008

Accepted 7 July 2008

Available online 16 July 2008

#### Keywords:

Poly(vinylidene fluoride)

Crystallization

Polymorphism

### ABSTRACT

A systematic study was carried out to investigate the effect of solvent type and temperature on the formation of the  $\alpha$  and  $\beta$  phases from solution cast PVDF. Three solvents with different boiling points were used: *N,N*, dimethylformamide (DMF), *N*-methyl-2-pyrrolidone (NMP) and hexamethylphosphoramide (HMPA). Infrared spectroscopy (FTIR) and scanning electron microscopy (SEM) revealed that the type of phase formed depends on the crystallization rate of PVDF, which in turn is determined by the evaporation rate of the solvent. Low rates result predominantly in the *trans*-planar  $\beta$  phase, high rates predominantly in the *trans-gauche*  $\alpha$  phase and intermediate rates in a mixture of these two phases, regardless of solvent and temperature used. Since evaporation rate of the solvent is intimately related to temperature, PVDF films can be obtained predominantly in either one of these phases, or a mixture of these, by an adequate choice of the evaporation temperature range for a given solvent. The possible solubility curves of the two polymorphs  $\alpha$  and  $\beta$  of PVDF were sketched. The formation of different types of spherulites, associated with the two different PVDF polymorphs, could be verified by surface micrographs of the cast films.

© 2008 Elsevier Ltd. All rights reserved.

### 1. Introduction

PVDF is a widely investigated semicrystalline polymer because of its broad spectrum of applications [1,2]. A fascinating characteristic of this polymer is its polymorphism, i.e., the possibility to form different crystalline structures. Depending on the crystallization conditions this polymer may present at least four different well-known crystalline structures: the orthorhombic  $\alpha$ ,  $\beta$  and  $\delta$  phases, and the monoclinic  $\gamma$  phase. The nonpolar  $\alpha$  phase, most readily obtained from the melt, has a *trans-gauche* conformation ( $TG^+TG^-$ ). The polar  $\beta$  phase, with improved pyro and piezoelectric properties, has an all *trans* planar zigzag conformation (TTT). The polar  $\gamma$  phase, obtained from high-temperature crystallization, has a conformation intermediate between that of the  $\alpha$  and the  $\beta$  phases, consisting of a sequence of three *trans* linked to a *gauche* ( $TTTG^-TTTG^+$ ). The  $\delta$  phase is a polar version of the  $\alpha$  phase and is obtained by polarizing an originally  $\alpha$ -phase sample in a high electric field (1.25 MV/cm) [3]. The  $\alpha$  crystal has a dipole moment of 1.2 D normal to the chains and of 1.02 D in the direction of the chains. The  $\beta$  crystal has a dipole moment of 2.1 D essentially normal to the chain direction. Conversion between the distinct

PVDF phases may occur by convenient thermal, mechanical or electric treatments.

In certain applications it may be very important to obtain a specific polymorph under controlled and reproducible conditions. Therefore, in recent years many investigations have been conducted regarding the effect of solvent type, humidity, concentration, temperature, substrate, and the addition of PMMA on the formation of the polymorphs of solution cast PVDF [4–14]. Some of these studies dealt with the production of membranes, using solvent mixtures and phase inversion techniques [11,15]. However, the effect of solvent type and temperature on the formation of the PVDF polymorphs has been the subject of much controversy and little is known on how to control the formation of a specific crystalline phase through convenient choice of solvent and crystallization temperature. In a previous work [16] it has been demonstrated that the type of predominant phase strongly depends on the evaporation temperature of the solvent. Temperatures below 70 °C provided exclusively the  $\beta$  phase. At increasing temperatures formation of the  $\alpha$  phase commenced and became predominant above 110 °C. However, only one solvent, dimethylacetamide (DMA), was used in that work and the indicated temperatures were specific for this solvent.

The objective of the current work is to verify the effect of the solvent properties and temperature on the formation of each crystalline phase of PVDF, utilizing several solvents with distinct boiling points. Since different boiling points result in different

<sup>\*</sup> Corresponding author. Tel.: +55 1633518526; fax: +55 1633615404.  
E-mail address: [gregorio@power.ufscar.br](mailto:gregorio@power.ufscar.br) (R. Gregorio Jr.).

evaporation rates and, consequently, in different crystallization rates of PVDF, this work also verified the effect of crystallization rate on the formation of the PVDF polymorphs. The results provided important information about the relationship between solvent type and crystallization temperature range required to produce predominantly and reproducibly a specific crystalline phase of PVDF.

## 2. Experimental

The PVDF powder used was Forafon F4000HD from Elf Atochem. The melt temperature and crystallinity degree of the as-received resin were obtained by calorimetric measurements using a Q100 differential scanning calorimeter (DSC) from TA Instruments in  $N_2$  atmosphere and heating rate of  $10\text{ }^\circ\text{C}/\text{min}$ . The degree of crystallinity was calculated from the melt enthalpy, using an equilibrium melt enthalpy of  $104.6\text{ J/g}$  for the  $\alpha$  phase [17]. The organic solvents used were: acetone (Merck, 99.7%), *N,N*-dimethylformamide (DMF, Merck, 99.5%), *N*-methyl-2-pyrrolidone (NMP, Mallinckrodt, 98%) and hexamethylphosphoramide (HMPA, Fluka, 98%). These solvents were chosen because of their distinct boiling points ( $T_b$ ) and for being, with the exception of acetone, good solvents of PVDF [18]. Acetone is considered as a good swelling agent of PVDF, because at  $60\text{ }^\circ\text{C}$  it swells and partially dissolves PVDF; however, at lower temperatures precipitation occurs. Thermogravimetric analyses of the solution were carried out in a 2950 TGA HR V5.4A equipment from TA Instruments, in the temperature range between 30 and  $250\text{ }^\circ\text{C}$  and at a heating rate of  $10\text{ }^\circ\text{C}/\text{min}$ . Infrared spectra (FTIR) were obtained using a Perkin-Elmer Spectrum 1000 spectrophotometer with resolution of  $2\text{ cm}^{-1}$  and diaphragm diameter of 2 mm. Scanning electron micrographs (SEM) were obtained using a Philips XL30-FEG microscope.

PVDF was dissolved in the different solvents at  $60\text{ }^\circ\text{C}$  for 6 h under continuous agitation using a magnetic stirrer in a hermetically sealed glass flask. Initial concentration of the solution was 5 wt%. The acetone solution, even after stirring at  $60\text{ }^\circ\text{C}$  for 12 h, did not become homogeneously transparent. The solutions were afterwards kept at a specific temperature, denominated the solvent evaporation temperature,  $T_s$ , for 30 min, sufficient for reaching thermal equilibrium. After this period the solution was spread on a previously cleaned glass substrate kept on a hot plate at temperature  $T_s$ . The whole system remained at this temperature for 30 min in a closed hood provided with exhaustion. This time was sufficient for complete evaporation of the solvent and formation of sustainable films with approximate dimensions of  $3\text{ cm} \times 4\text{ cm} \times 5\text{ }\mu\text{m}$ .  $T_s$ s used were 30, 40 and  $50\text{ }^\circ\text{C}$  for the acetone solution and 60, 80, 100, 120 and  $140\text{ }^\circ\text{C}$  for the DMF, NMP and HMPA solutions. These temperatures were chosen to avoid reaching the boiling points of the solvent and the onset of polymer melting. Next, the films were removed from the substrate by immersing in distilled water, and then kept at  $60\text{ }^\circ\text{C}$  for 12 h in an oven for drying and removal of possible solvent residues. The heating plate used was constructed in our laboratory and allows temperature control with maximum variation of  $2\text{ }^\circ\text{C}$  in a  $36\text{ cm}^2$  area. Films were maintained in the center of this region.

## 3. Results

The DSC curve (heating) of the PVDF resin used is shown in Fig. 1. The melt endotherm has a peak at  $168\text{ }^\circ\text{C}$ , with onset at approximately  $140\text{ }^\circ\text{C}$ . This onset temperature was used as limit for  $T_s$ . The degree of crystallinity was calculated as 49%. The predominant crystalline phase in this resin was  $\alpha$ , as verified by FTIR.

Some properties of the solvents used are presented in Table 1.

Acetone is considered as a good swelling agent of PVDF [18] and at room temperature ( $20\text{ }^\circ\text{C}$ ) the interaction energy between the

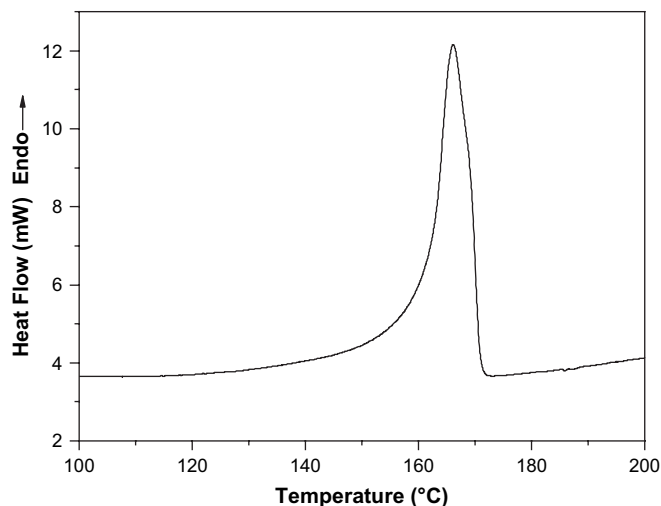


Fig. 1. DSC curve of the PVDF resin used.

Table 1

Properties of the solvents used

Solvent	Formula	Density at $20\text{ }^\circ\text{C}$ (g/mL)	Boiling point, $T_b$ ( $^\circ\text{C}$ )	Dipole moment at $20\text{ }^\circ\text{C}$ (D)	Vapor pressure at $25\text{ }^\circ\text{C}$ (Pa)
Acetone	$C_3H_6O$	0.786	56.2	2.85	24 280
DMF	$C_3H_7NO$	0.944	153	3.86	490
NMP	$C_5H_9NO$	1.033	202	4.09	45
HMPA	$C_6H_{18}N_3OP$	1.03	235	5.54	9.3

polymer chains is higher than the polymer/solvent interaction energy. Thus, the crystalline region of PVDF remains practically intact and only swelling results, as the solvent manages to penetrate the amorphous region. At increasing temperature the interaction energy between polymer chains decreases and the solvent manages to penetrate the crystalline region, causing complete or partial dissolution. In the current work the PVDF/acetone solution was kept at  $60\text{ }^\circ\text{C}$  for 12 h under stirring in a hermetically closed glass vessel. After this period of time the solution still did not show complete transparency. The solutions with the other solvents, considered good solvents of PVDF [18], after 6 h stirring at  $60\text{ }^\circ\text{C}$  showed to be completely transparent, confirming complete dissolution of the polymer.

Results of thermogravimetric (TG) analyses of the solvents used at 5 wt% solution are shown in Fig. 2. The aim of these analyses was to observe the evaporation behavior of the different solvents as a function of temperature. Acetone was not analyzed, because it is not good solvent of PVDF, as will be shown next. Evaporation of DMF, NMP and HMPA starts at approximately 30, 40 and  $50\text{ }^\circ\text{C}$ , respectively. The derivative of the TG curves, i.e., DTG, provides the variation of the evaporation rate of the solvent as a function of temperature, as shown in Fig. 3.

As expected, solvents with higher  $T_b$  start evaporating at higher temperature and present lower evaporation rate at a given temperature. In the film forming process the evaporation rate of the solvent is proportional to the crystallization rate of the polymer. So, at a given temperature the crystallization rate of PVDF will be inversely proportional to  $T_b$  and directly proportional to the vapor pressure of the solvent used.

Figs. 4–7 show the infrared spectra (FTIR) of the films crystallized at different temperatures and from different solvent solutions. The characteristic bands of the  $\alpha$  and  $\beta$  phases are indicated in the figures.

The crystalline phases of PVDF can be characterized by the infrared absorption bands between  $400$  and  $1000\text{ cm}^{-1}$  [1,10,16,19–22].

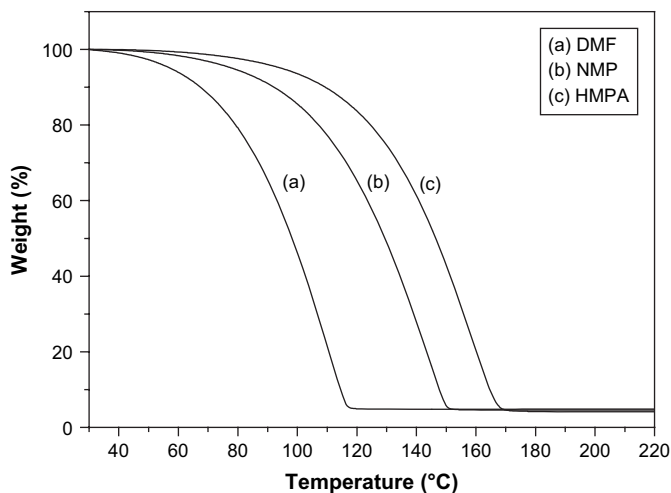


**Fig. 2.** Results of thermogravimetric analyses of the solvents: (a) DMF, (b) NMP and (c) HMPA. Solutions at initial concentration of 5 wt% and mass of  $\approx 27$  mg. Heating rate of  $10^\circ\text{C}/\text{min}$ .

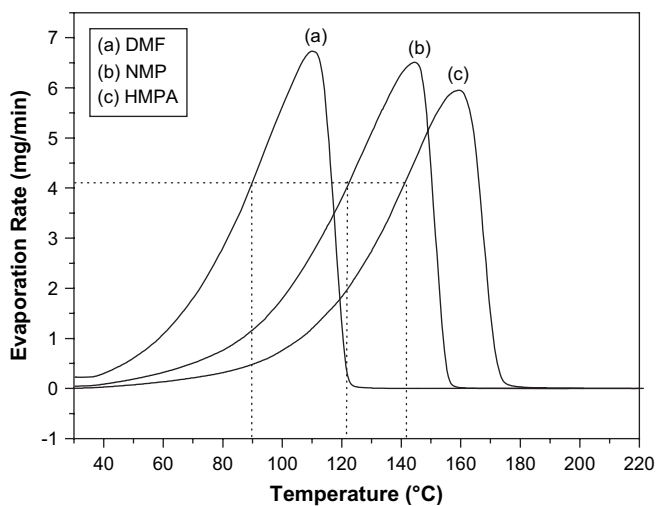


**Fig. 3.** Variation of the evaporation rate as a function of temperature for the three solvents: (a) DMF, (b) NMP and (c) HMPA.

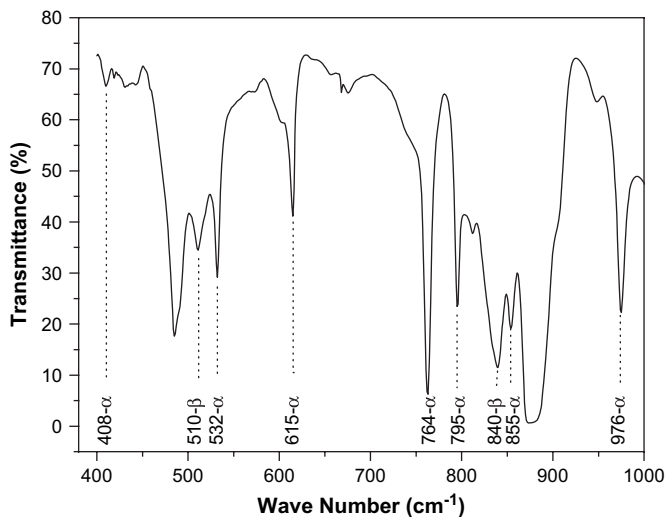


**Fig. 4.** Spectrum of the films cast from acetone solution.

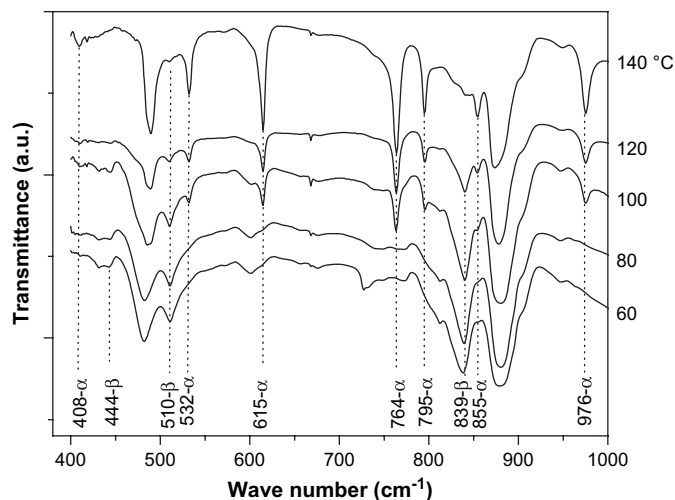


**Fig. 5.** FTIR spectra of the films cast from DMF solution at different temperatures.

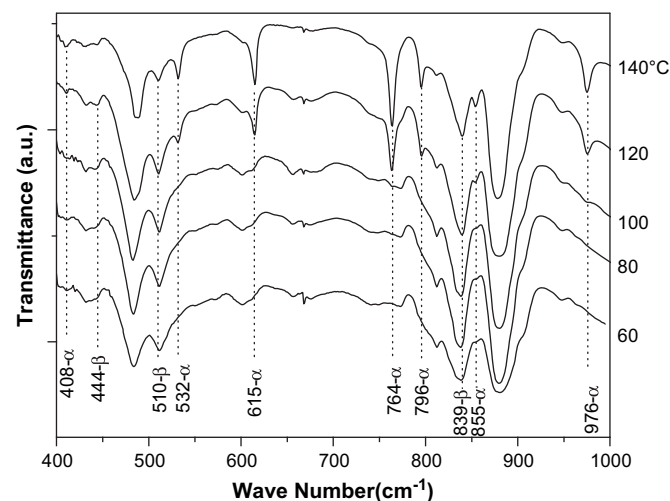


**Fig. 6.** FTIR spectra of the films cast from NMP solution at different temperatures.

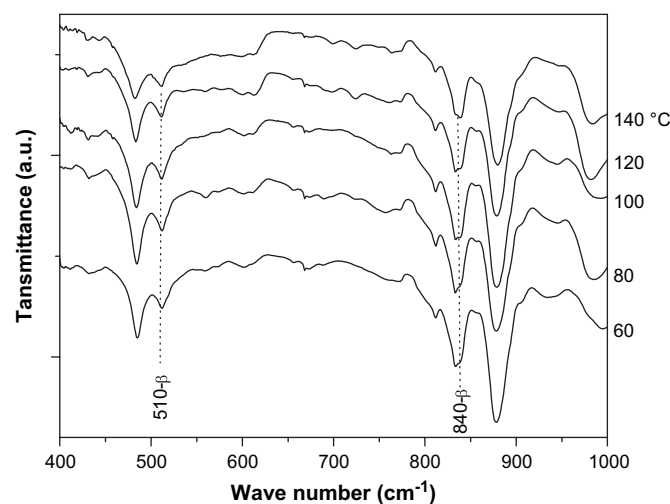


**Fig. 7.** FTIR spectra of the films cast from HMPA solution at different temperatures.

The bands at 485 and 879  $\text{cm}^{-1}$  are attributed to the amorphous phase of PVDF, and can therefore not be used to identify any of the crystalline phases. The bands at 408, 532, 614, 764, 796, 855 and 976  $\text{cm}^{-1}$  are associated with the  $\alpha$  phase of PVDF. The bands at 444 and 510  $\text{cm}^{-1}$  are characteristic of the  $\beta$  phase and those at 431, 512, 776, 812 and 833  $\text{cm}^{-1}$  are related to the  $\gamma$  phase. The 840  $\text{cm}^{-1}$  band is common to the  $\beta$  and  $\gamma$  phases; a sharp and well-resolved band indicates the  $\beta$  phase, whereas a broad band indicates the  $\gamma$  phase. This broad band is due to overlapping with the 833  $\text{cm}^{-1}$  band which frequently appears as a shoulder [22,23].

Films crystallized from acetone solution at 30, 40 and 50 °C presented very similar spectra, of which a representative is shown in Fig. 4. All spectra showed predominance of the  $\alpha$  phase with a minor amount of the  $\beta$  phase. Since the PVDF resin used presents almost exclusively the  $\alpha$  phase, it is very likely that the polymer crystals were only partially dissolved by acetone and part of the resulting  $\alpha$  phase is the original phase itself. The crystalline part dissolved by acetone likely crystallized as a mixture of  $\alpha$  and  $\beta$ , resulting in a minor part of the latter. So, since acetone is not a good solvent of PVDF, little and imprecise information can be obtained regarding the type and amount of phase formed during crystallization from acetone solution.

The films crystallized from DMF solution (Fig. 5) contain predominantly the  $\beta$  phase for  $T_s \leq 80$  °C. At 90 °C the evaporation rate of the solvent is 4.1 mg/min (Fig. 3), which is assumed to be approximately the rate necessary for the onset of  $\alpha$  phase formation. At increasing  $T_s$  the amount of formed  $\alpha$  phase increases up to  $T_s = 140$  °C where this phase becomes almost exclusive. These results are similar to those obtained in previous works, where DMF or DMA was used as solvent [10,16];  $T_b$  of these solvents is very close (DMA has  $T_b = 165$  °C and DMF has  $T_b = 153$  °C). Films prepared from NMP (Fig. 6) contain predominantly the  $\beta$  phase at  $T_s \leq 100$  °C. Above this temperature formation of  $\alpha$  phase will start. The amount of  $\alpha$  phase increases as temperature is increased; however, even at 140 °C there is still a large amount of  $\beta$  phase present. It can be seen from Fig. 3 that NMP evaporates at the required rate for  $\alpha$  phase formation of 4.1 mg/min only close to 120 °C. At this temperature there is already a certain amount of  $\alpha$  phase in the sample (Fig. 6), indicating that in this case the required evaporation rate is likely a little lower. In the samples prepared from HMPA (Fig. 7), at all temperatures only the  $\beta$  phase was formed. In fact, this solvent reaches the evaporation rate of 4.1 mg/min only above 140 °C (Fig. 3). In Figs. 6 and 7 a weak band at 812  $\text{cm}^{-1}$  can be seen, which also appears in Fig. 5 at the temperatures of 60 and 80 °C, however, less intense. The appearance of this band might indicate the existence of a small amount of  $\gamma$  phase or that this band is common to the  $\beta$  phase. It should be pointed out that weak bands like these ones are frequently related to small inclusions of a specific crystalline phase in the sample and of which the detection depends on the sample region that is analyzed and on the diameter of the spectrophotometer diaphragm used [23]. Small diameters, of the same order of the inclusions, allow determination of the existence of these inclusions, as well as detection of closely lying bands, like those at 833 and 840  $\text{cm}^{-1}$  of the  $\gamma$  phase. Spectra of the films crystallized from HMPA solution (Fig. 7) also display a broad band near 990  $\text{cm}^{-1}$ , characteristic of HMPA, indicating incomplete solvent removal from the samples, even after 12 h at 60 °C in an oven.

Surface micrographs of the samples crystallized at different temperatures and from different solvents are shown in Figs. 8–13. Micrographs were obtained from the free surface of the samples, i.e., opposite to the surface in contact with the glass substrate.

The films crystallized from acetone solution displayed similar morphology at the three temperatures: 30, 40 and 50 °C. A representative micrograph is shown in Fig. 8. PVDF is known to present a morphology consisting of spherulites when crystallized from solution or from the melt. However, the morphology of acetone cast

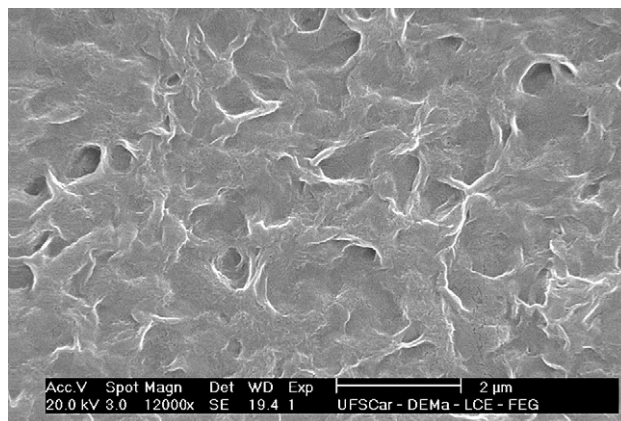
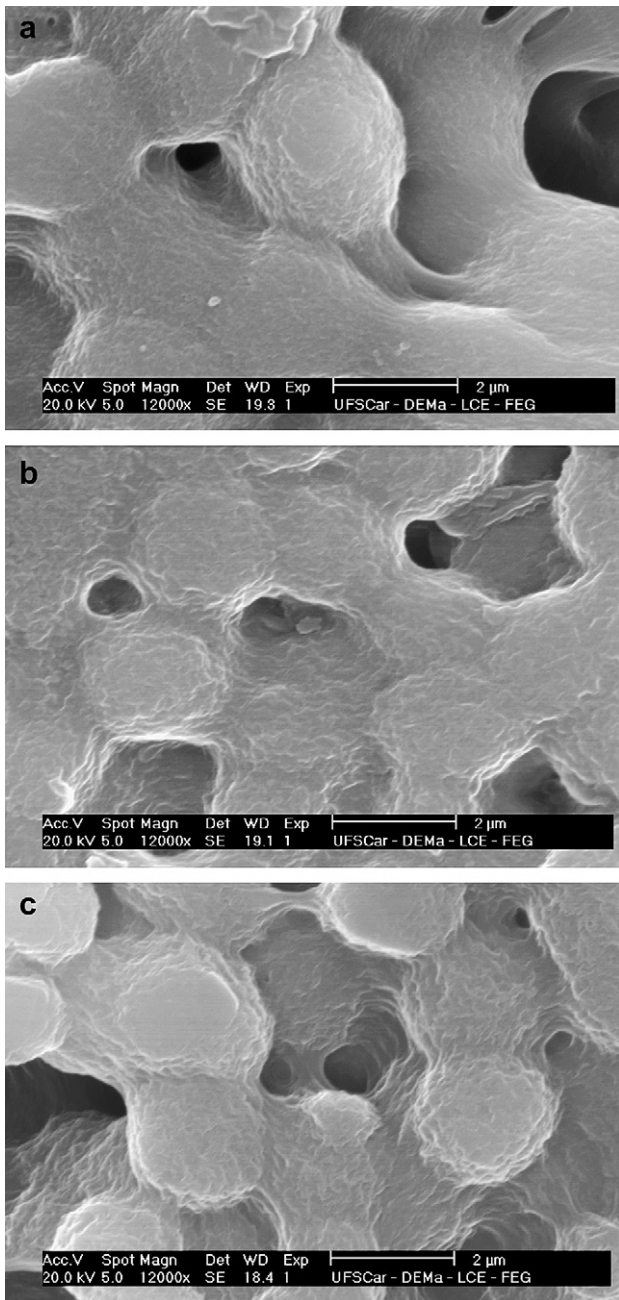


Fig. 8. SEM micrographs of the surface of the films cast from acetone solution at 30, 40 and 50 °C.

films consists of randomly interlinked lamellae, indicating that acetone penetrated into the amorphous phase of PVDF and destroyed the typical spherulitic structures of this polymer. Since likely only a small part of the crystalline region was dissolved and little crystallization occurred during solvent evaporation, no new spherulites were formed. This result confirms the results obtained from FTIR, i.e., acetone did not completely dissolve PVDF and no predominant crystalline phases were formed during solvent evaporation. Therefore, acetone will not be used in the investigation of the effect of solvent and temperature on the crystalline phases formed. However, the assumption made in a previous work [10] is confirmed, i.e., when a good swelling agent is used in solution crystallization of PVDF only part of the crystalline region will be dissolved and the resulting crystalline phases will be a mixture of the phase present in the resin and of those formed during solvent evaporation.

Films crystallized at 60 °C from DMF solution displayed spherulites with average diameter of 3  $\mu\text{m}$ , whereas those crystallized from NMP and HMPA solutions presented average diameter of 2.5  $\mu\text{m}$ . Sample porosity showed to be proportional to solvent boiling point, i.e., the lower the evaporation rate of the solvent the higher the sample porosity. At 80 °C the spherulite diameter in the DMF cast films decreased to 2.7  $\mu\text{m}$  and porosity was reduced. In the NMP cast films the spherulites maintained practically the same size and in the HMPA cast films they increased to 3  $\mu\text{m}$ . In both cases porosity was slightly reduced and remained proportional to the boiling point of the solvent. At 100 °C the film crystallized from DMF solution showed lower porosity, spherulites with average diameter of 5  $\mu\text{m}$  and radial lamellae between the spherulites. This was the temperature at which the FTIR spectra started indicating the formation of the  $\alpha$  phase (Fig. 5, 100 °C), and these radial lamellae are therefore likely related to this phase. So, from now on the spherical structures will be denominated as  $\beta$  spherulites and the radial lamellae as  $\alpha$  spherulites. The films crystallized from NMP and HMPA solutions presented only  $\beta$  spherulites with average diameter of 4  $\mu\text{m}$  and high porosity still. At this temperature no radial lamellae were seen between the spherulites. At 120 °C the film crystallized from DMF solution presented predominantly  $\alpha$  spherulites, with average diameter of 6–7  $\mu\text{m}$ , few  $\beta$  spherulites and practically no porosity. NMP cast films presented 7–8  $\mu\text{m}$   $\beta$  spherulites with some  $\alpha$  spherulites between these. The FTIR spectrum of this film indeed shows the beginning of the formation of the  $\alpha$  phase (Fig. 6, 120 °C). The HMPA cast films only presented 6–7  $\mu\text{m}$   $\beta$  spherulites, in agreement with the results obtained by FTIR (Fig. 7). The NMP and HMPA cast films remained porous. At 140 °C the DMF cast samples contained only  $\alpha$  spherulites of approximately 12  $\mu\text{m}$ , the NMP



**Fig. 9.** SEM micrographs of the surfaces of films cast at 60 °C from DMF (a) NMP (b) and HMPA (c) solutions.

ones a mixture of  $\alpha$  and  $\beta$  spherulites of about 10–12  $\mu\text{m}$  and the HMPA ones only  $\beta$  spherulites of about 12  $\mu\text{m}$ . The DMF cast sample presented almost no porosity and the NMP cast sample little porosity. The HMPA cast sample remained very porous and the spherulites presented small voids on the surface. All these results are in agreement with FTIR results.

The increase in temperature and, consequently, increase in crystallization rate, resulted in slightly larger spherulites. This fact can be explained in terms of the PVDF crystallization rate, which has a maximum close to 145 °C [28] and therefore we are in the region where the crystallization rate increases with increasing temperature (between 60 and 140 °C), due to the increase in growth rate and reduction in nucleation rate. This results in an increase in spherulite size as crystallization temperature increases.

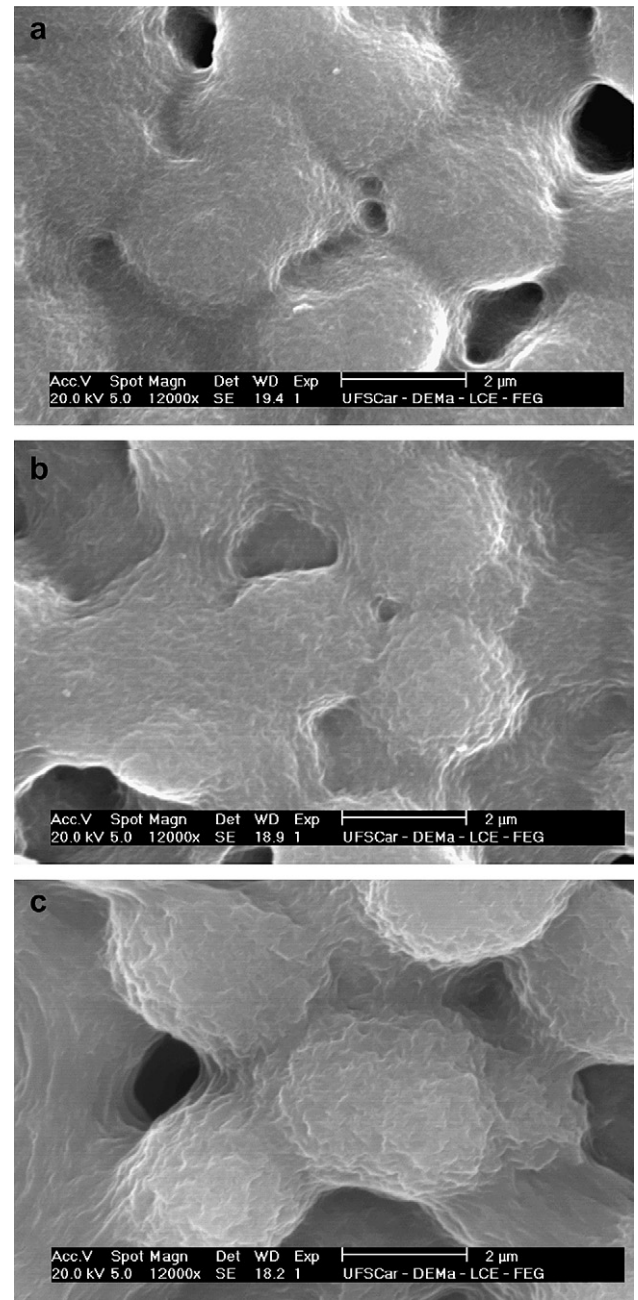


**Fig. 10.** SEM micrographs of the surfaces of films cast at 80 °C from DMF (a) NMP (b) and HMPA (c) solutions.

#### 4. Discussion

The mechanism behind solution crystallization of polymers is very complex and still little is known on molecular level. The crystallization rate is intimately related to the evaporation rate of the solvent, which in turn depends on the boiling point (which is proportional to the intensity of the dipole moment of the molecules) and on the temperature at which crystallization occurs. The results obtained in this work indicate that the resulting crystalline phase depends on the crystallization rate. Low rates result predominantly in the *trans*-planar  $\beta$  phase, high rates predominantly in the *trans-gauche*  $\alpha$  phase and intermediate rates in a mixture of these two, regardless of the solvent or temperature used. Low crystallization rates favor the *trans* conformations and high rates favor the *gauche* conformations. Such behavior was previously suggested by Tashiro

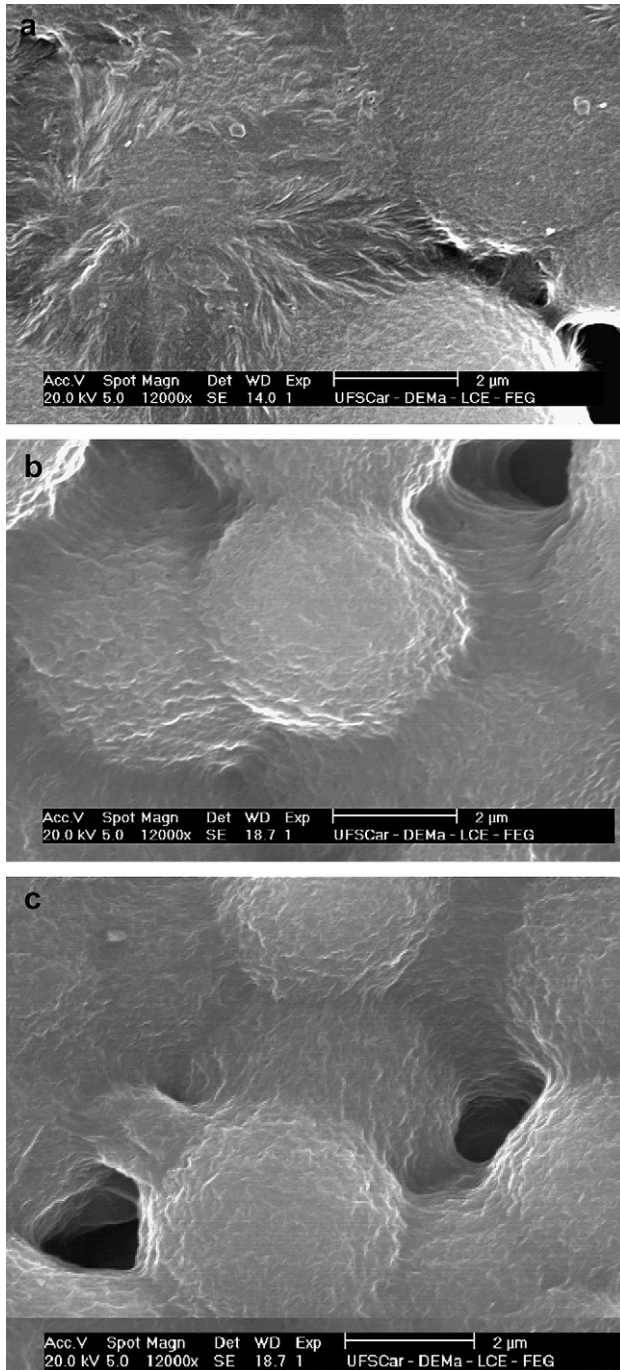


**Fig. 11.** SEM micrographs of the surfaces of films cast at 100 °C from DMF (a) NMP (b) and HMPA (c) solutions.

[1]. To confirm this tendency, a sample was crystallized from DMF solution at 140 °C, under the same previous conditions, however, covered with an 80 cm<sup>3</sup> glass bell jar. In this manner, the solvent evaporated in a saturated atmosphere, reducing the evaporation rate. The FTIR spectrum of this film is shown in Fig. 14. For comparison sake, the spectrum of the sample crystallized under the same conditions but without the bell jar (same spectrum of Fig. 5, 140 °C) was also included. The micrograph of the film surface is shown in Fig. 15.

The FTIR spectra show that in the film crystallized at 140 °C under the bell jar,  $\alpha$  and  $\beta$  phases were formed with predominance of the latter. In the absence of the bell jar only the  $\alpha$  phase was formed. The micrograph of the film crystallized under the bell jar

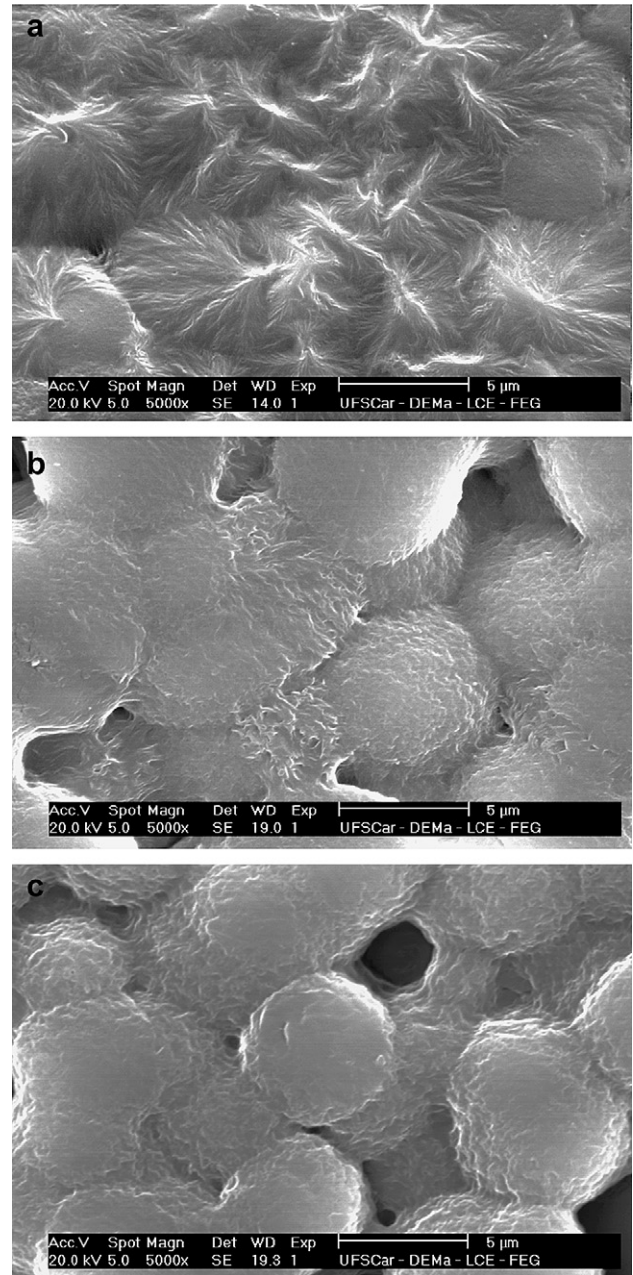


**Fig. 12.** SEM micrographs of the surfaces of films cast at 120 °C from DMF (a) NMP (b) and HMPA (c) solutions.

shows a morphology composed predominantly of  $\beta$  spherulites and small formations of  $\alpha$ , confirming the FTIR results. This experiment confirms that for a same solvent and a same temperature, reduction in the solvent evaporation rate and, consequently, the crystallization rate of PVDF, favors the formation of the *trans* phase. It is also interesting to note that the film crystallized under the bell jar presented a band at 812 cm<sup>-1</sup> with an intensity stronger than that seen in the NMP and HMPA solution cast samples (Figs. 6 and 7), as discussed previously. In addition, a band at 431 cm<sup>-1</sup> is also seen, considered characteristic of the  $\gamma$  phase. Formation of this phase is possible, considering the fact that in its conformation *trans* bonds (TTTG<sup>-</sup>TTTG<sup>+</sup>) also prevail, despite previous studies [10,16,21,22,24] showing that this phase only is formed near  $T_m$  of PVDF. Moreover, the DSC curve of this sample (not shown) did not display the melt endotherms corresponding to this phase, with peaks at about 179 and 188 °C [10,22]. Only one endotherm was observed with peak at

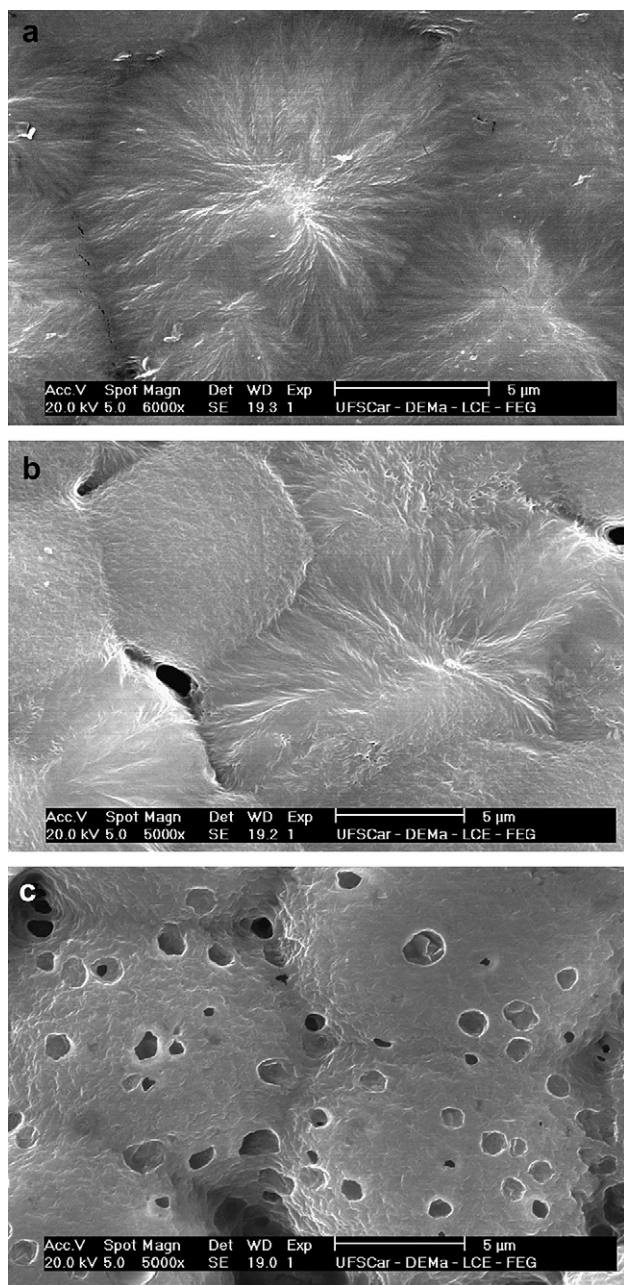


**Fig. 13.** SEM micrographs of the surfaces of films cast at 140 °C from DMF (a) NMP (b) and HMPA (c) solutions.

168 °C, corresponding to the melt of the  $\alpha$  and  $\beta$  crystals [10,16]. The low evaporation rate favored the formation of the  $\beta$  phase, however, at high temperature it might have allowed the formation of some *gauche* conformations, resulting in  $TG^+TG^-$  and  $TTTG^-TTTG^+$  sequences, and consequently, in the characteristic bands of the  $\alpha$  and  $\gamma$  phases. However, it is most likely that the bands at 431 and 812  $\text{cm}^{-1}$  are common to the  $\beta$  and  $\gamma$  phases, being more intense in the samples where the  $\gamma$  phase, formed from the  $\alpha \rightarrow \gamma$  phase transformation [10], predominates. Hence, in solution crystallization of PVDF it seems that the resulting crystalline phase is determined neither by the type of solvent nor by the evaporation temperature, but by the crystallization rate. An explanation for this behavior might be given considering that in PVDF the  $\beta$  phase is thermodynamically more favorable, whereas the  $\alpha$  phase is kinetically more favorable [1,25]. When crystallization rate is slow, the chains can relax and form the thermodynamically more favorable

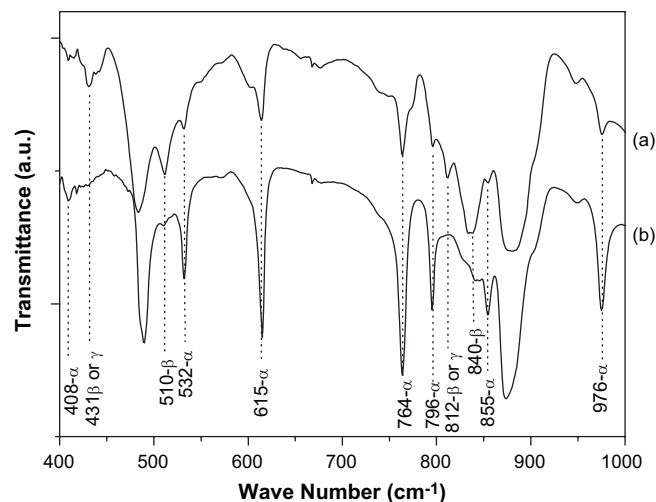


**Fig. 14.** FTIR spectra of the films cast from DMF solution at 140 °C under the bell jar (a) and without the bell jar (b).

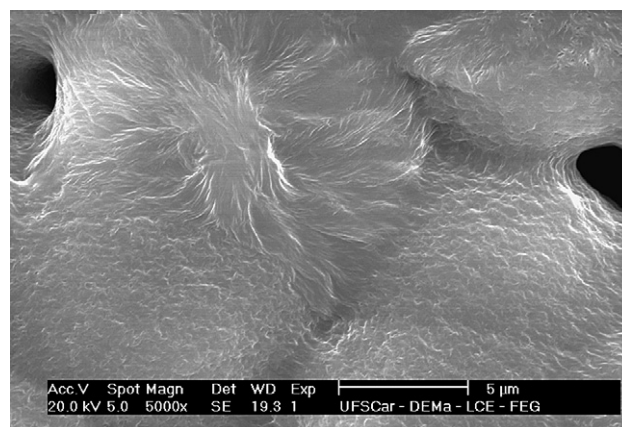


**Fig. 15.** SEM micrograph of the surface of film cast from DMF solution at 140 °C under the bell jar.

*trans* conformation. On the contrary, when crystallization rate is fast, the entropically more favorable conformation does not have sufficient time and thermal energy to form and prevail the kinetically more favorable *gauche* conformation. In very thick samples, where the solvent evaporation rate at the surface and in the bulk can be very different, formation of different amounts of each crystalline phase may occur throughout sample thickness. Relative humidity and solution concentration also interfere in solvent evaporation rate and will, consequently, influence the type of phase formed.

The results obtained also allowed to sketch the possible solubility curves of the two PVDF polymorphs, shown in Fig. 16.

The solid lines represent the solubility curves of the  $\alpha$  and  $\beta$  polymorphs and the dashed lines represent the limits of the metastable zones of the two phases. The intersection of the two solubility curves yields the transition temperature ( $T_x$ ) between the two forms. When an unsaturated solution with a given initial concentration is maintained at a temperature below  $T_1$ , evaporation of the solvent will increase the concentration until it surpasses the solubility curve of the  $\beta$  polymorph and reaches the metastable zone (point  $P_1$ ). At this point nucleation and growth of the  $\beta$  phase occur spontaneously and this will be the predominant phase. If the solution is maintained at a temperature between  $T_1$  and  $T_x$ , concentration will cross the  $\alpha$  phase solubility curve before reaching the limit of the  $\beta$  metastable zone (point  $P_2$ ) and both forms may

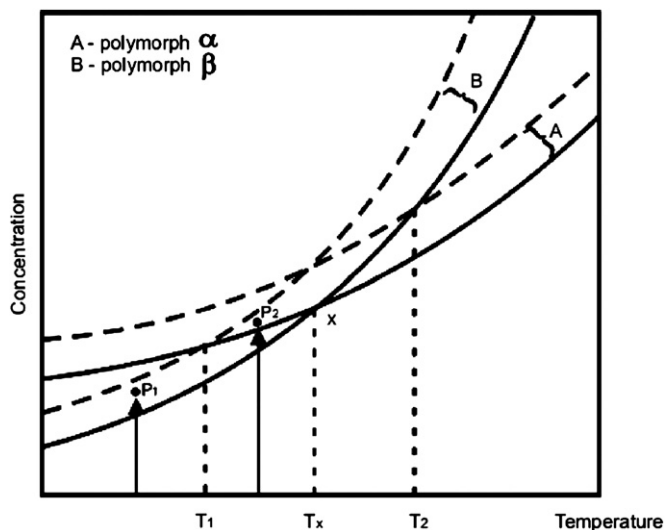


Fig. 16. Solubility curves of the two polymorphs  $\alpha$  and  $\beta$  of PVDF, adapted from Ref. [26]. The dashed lines represent the limits of the metastable zones of the two phases.

nucleate and grow, resulting in a mixture of the  $\alpha$  and  $\beta$  phases. The closer to temperature  $T_x$  the higher the amount of formed  $\alpha$  phase. At the transition temperature  $T_x$  approximately equal amounts of the two phases will form, if the nucleation and growth rate of the two phases are similar. Temperatures between  $T_x$  and  $T_2$  also result in a mixture of the two phases, with predominance of the  $\alpha$  phase, of which the amount increases with temperature. Above  $T_2$  only  $\alpha$  phase is predominantly formed. Solvents with different boiling points and, consequently, distinct evaporation rates, present different temperatures  $T_1$ ,  $T_2$  and  $T_x$ . The result obtained in the present work shows that for DMF,  $T_1 \approx 80^\circ\text{C}$ ,  $T_x \approx 100^\circ\text{C}$  and  $T_2 \approx 130^\circ\text{C}$ . For NMP,  $T_1 \approx 100^\circ\text{C}$ ,  $T_x \approx 120^\circ\text{C}$  and  $T_2 > 140^\circ\text{C}$  and for HMPA  $T_1 > 140^\circ\text{C}$ . The relation between these temperatures for the three solvents is proportional to the relation between their boiling points. The initial concentration of the solution should affect the process, as it also alters the crystallization rate.

In the isothermal crystallization of polymers from the melt, crystallization kinetics is sensitive to small temperature variations. Temperatures close to  $T_m$  of the polymer reduce the crystallization rate by reducing the nucleation and growth of the crystallites. For PVDF these temperatures favor the *trans* conformation, through crystallization of the  $\gamma$  phase and the  $\alpha \rightarrow \gamma$  phase transition [10,16,21,22,24]. When the temperature is reduced crystallization rate increases, favoring the *gauche* conformation and the  $\alpha$  phase is predominantly formed. So, in melt crystallization the crystallization rate also seems to determine the phase that will be formed. Apparently low crystallization rates favor formation of the thermodynamically more favorable *trans* conformations, and high rates favor the kinetically more favorable *gauche* conformations. Some works have shown that in PVDF/PMMA blends, with 10–20% PMMA, the  $\beta$  phase may be formed by quenching from the melt [27–29]. This probably occurs because PMMA acts as a diluent and reduces the crystallization rate of PVDF, favoring crystallization of the *trans* conformation.

In the preparation of membranes by the phase inversion technique [15], where the polymer/solvent solution is spread on a substrate and subsequently immersed in a nonsolvent, solvent removal increases and, consequently crystallization of the polymer, of which the intensity depends on the temperature of the nonsolvent. Buonomenna et al. [11] observed that, when a 12 wt% PVDF/DMF solution was spread on a substrate and immersed in a coagulation

bath (water), the resulting crystalline phase depended on the water temperature. FTIR and XRD analyses revealed that at  $T = 25^\circ\text{C}$  the  $\beta$  phase predominated and at  $T = 60^\circ\text{C}$  the  $\alpha$  phase predominated. Our results showed that in the crystallization from PVDF/DMF solution  $\alpha$  phase only predominates when the evaporation temperature exceeds  $120^\circ\text{C}$  (Fig. 5). In the work of Buonomenna et al. the coagulation bath at  $60^\circ\text{C}$  accelerated the solvent withdrawal process and, consequently, the crystallization rate, resulting predominantly in the  $\alpha$  phase, even at that temperature. At coagulation at  $25^\circ\text{C}$  mass transfer by diffusion of the solvent and nonsolvent was slower, resulting in a lower crystallization rate and, consequently, in predominant formation of the  $\beta$  phase. Therefore, crystallization of PVDF by the phase inversion technique also corroborates our results, i.e., the resulting crystalline phase depends on solvent removal rate, which is intimately related to the crystallization rate of PVDF.

## 5. Conclusions

In the solution crystallization of PVDF, the resulting crystalline phase depends on the crystallization rate, which in turn is determined by the evaporation rate of the solvent. Low rates favor the formation of the *trans-planar*  $\beta$  phase, high rates result predominantly in the formation of the *trans-gauche*  $\alpha$  phase and intermediate rates allow formation of both phases. Thus, it is possible to produce predominantly and reproducibly a specific crystalline phase of PVDF, by controlling the evaporation rate of the solvent, as long as a good solvent of PVDF is used. Results also showed that these polymorphs are likely associated with spherulites of different lamellar structures.

## Acknowledgment

The authors thank FAPESP and CNPq for their financial support.

## References

- [1] Tashiro K. Crystal structure and phase transition of PVDF and related copolymers. In: Nalwa HS, editor. Ferroelectric polymers. New York: Marcel Dekker; 1995.
- [2] Chen QX, Payne PA. Meas Sci Technol 1995;6:249–67.
- [3] Davis GT, McKinney JE, Broadhurst MG, Roth SC. J Appl Phys 1978;49(10):4998–5002.
- [4] Benz M, Euler WB. J Appl Polym Sci 2003;89:1093–100.
- [5] Boccaccio T, Bottino A, Capannelli G, Piaggio P. J Membr Sci 2002;210:315–29.
- [6] Benz M, Euler WB, Gregory OJ. Macromolecules 2002;35:2682–8.
- [7] Kim KM, Jeon WS, Park NG, Ryu KS, Chang SH. Korean J Chem Eng 2003;20(5):934–41.
- [8] Salimi A, Yousefi AA. J Polym Sci Part B Polym Phys 2004;42:3487–95.
- [9] Park YJ, Kang YS, Park C. Eur Polym J 2005;41:1002–12.
- [10] Gregorio Jr R. J Appl Polym Sci 2006;100:3272–9.
- [11] Buonomenna MG, Macchi P, Davoli M, Drioli E. Eur Polym J 2007;43:1557–72.
- [12] Ma W, Zhang J, Wang X, Wang S. Appl Surf Sci 2007;253:8377–88.
- [13] Ma W, Zhang J, Wang X. J Macromol Sci Part B Phys 2008;47:139–49.
- [14] Ma W, Zhang J, Wang X. Appl Surf Sci 2008;254:2947–54.
- [15] Bottino A, Camara-Roda G, Capannelli G, Munari S. J Membr Sci 1991;57:1–20.
- [16] Gregorio Jr R, Cestari M. J Polym Sci Part B Polym Phys 1994;32:859–70.
- [17] Nakagawa K, Ishida Y. J Polym Sci Part B Polym Phys 1973;11(11):2153–71.
- [18] Bottino A, Capannelli G, Munari S. J Polym Sci Part B Polym Phys 1988;26:785–94.
- [19] Cortili G, Zerbi G. Spectrochim Acta 1967;23A:285–99.
- [20] Kobayashi M, Tashiro K, Tadokoro H. Macromolecules 1975;8(2):158–71.
- [21] Prest WM, Luca DJ. J Appl Phys 1975;46(10):4136–43.
- [22] Gregorio Jr R, Capitão RC. J Mater Sci 2000;35:299–306.
- [23] Bormashenko Y, Progreb R, Stanevsky O, Bormashenko E. Polym Test 2004;23:791–6.
- [24] Osaki S, Ishida Y. J Polym Sci Polym Phys Ed 1975;13:1071–83.
- [25] Lovinger AJ. In: Bassett DC, editor. Developments in crystalline polymers. London: Applied Science Publishers Ltd; 1982.
- [26] Threlfall T. Org Process Res Dev 2000;4(5):384–90.
- [27] Song D, Yang D, Feng Z. J Mater Sci 1990;25:57–64.
- [28] Gregorio Jr R, Nocite NCPS. J Phys D Appl Phys 1995;28:432–6.
- [29] Kim KJ, Cho YJ, Kim YH. Vib Spectrosc 1995;9:147–59.